Citation: Cell Death and Disease (2011) 2, e231; doi:10.1038/cddis.2011.118

www.nature.com/cddis

Disruption of a mitochondrial protease machinery in *Plasmodium falciparum* is an intrinsic signal for parasite cell death

S Rathore[1,2], S Jain[1,2], D Sinha[1,2], M Gupta[1], M Asad[1], A Srivastava[1], MS Narayanan[1], G Ramasamy[1], VS Chauhan[1], D Gupta[1] and A Mohmmed*[,1]

The ATP-dependent ClpQY protease system in *Plasmodium falciparum* is a prokaryotic machinery in the parasite. In the present study, we have identified the complete ClpQY system in *P. falciparum* and elucidated its functional importance in survival and growth of asexual stage parasites. We characterized the interaction of *P. falciparum* ClpQ protease (PfClpQ) and PfClpY ATPase components, and showed that a short stretch of residues at the C terminus of PfClpY has an important role in this interaction; a synthetic peptide corresponding to this region antagonizes this interaction and interferes with the functioning of this machinery in the parasite. Disruption of ClpQY function by this peptide caused hindrance in the parasite growth and maturation of asexual stages of parasites. Detailed analyses of cellular effects in these parasites showed features of apoptosis-like cell death. The peptide-treated parasites showed mitochondrial dysfunction and loss of mitochondrial membrane potential. Dysfunctioning of mitochondria initiated a cascade of reactions in parasites, including activation of VAD–FMK-binding proteases and nucleases, which resulted in apoptosis-like cell death. These results show functional importance of mitochondrial proteases in the parasite and involvement of mitochondria in programmed cell death in the malaria parasites.
Cell Death and Disease (2011) **2,** e231; doi:10.1038/cddis.2011.118; published online 24 November 2011
Subject Category: Internal Medicine

Malaria remains a major parasitic disease in the tropical and sub-tropical countries causing 1–2 million deaths globally every year.[1,2] The malaria parasite harbors two organelles of prokaryotic origin, the mitochondrion and the apicoplast. The metabolic pathways in these organelles are important for growth cycle and survival of the parasite.[3–5] Characterization of novel metabolic pathways in these organelles and understanding their functional role in parasite growth and survival may be a key step to design new anti-malarial strategies.

ATP-dependent protease machineries including the eukaryotic 26S proteasome and the prokaryotic casenolytic proteases (Clp) systems are large protein-degradation complexes that have an essential role in cell-cycle regulation.[6,7] The ClpQY machinery is a multimeric ATP-dependent protease system in prokaryotes that resembles the eukaryotic 26S proteasome; it consists of two stacked hexameric rings of ClpQ protease that are capped on one of both sides with a hexameric ring of AAA-type ATPase, ClpY.[8] The ATPases act as chaperons to unfold the substrate proteins, which subsequently get degraded by the protease component. Interaction of protease and ATPase components is essential for proper functioning of these protease machineries.[8,9]

The eukaryotic 26S proteasome machinery is an important regulatory system that controls level of key cell-cycle regulators and transcription factors;[7,10] Inhibition of the 26S proteasome dysregulates cell processes that leads to apoptosis of eukaryotic cells.[10–12] The ClpQY machinery shows mechanistic resemblance with 26S proteasome.[7] The ClpQY machinery is shown to regulate levels of cell division inhibitor and to function as an activator of capsular polysaccharide synthesis.[13]

The *P. falciparum* genome harbors two Clp protease systems, ClpQY and ClpAP. We have earlier characterized *P. falciparum* ClpQ (PfClpQ) protease and ClpP protease system.[14,15] The PfClpQ protease is localized in mitochondria whereas PfClpP is localized in apicoplast, relict plastid in the parasite.[15,16] Our interest in understanding functional importance of prokaryotic machineries in the parasite prompted us to assess possible functional role of the ClpQY machinery in the parasite. In the present study, we have functionally characterized complete ClpQY system in *P. falciparum*. Disruption of ClpQY activity using a small peptide that interferes with functioning of this machinery, caused dysregulation of mitochondrial functions, which in turn activated cascade of reactions leading to apoptosis-like cell death of the parasite. These results suggest role of mitochondrial proteases in maintenance of functional mitochondria and points towards involvement of mitochondria in apoptosis-like cell death in parasite.

[1]International Centre for Genetic Engineering and Biotechnology, New Delhi, India
*Corresponding author: A Mohmmed, International Centre for Genetic Engineering and Biotechnology, Aruna Asaf Ali Marg, New Delhi 110067, India.
Tel: +91 11 2674 1358; Fax: +91 11 2674 2316; E-mail: amohd@icgeb.res.in
[2]These authors contributed equally to this work.
Keywords: *Plasmodium*; ClpQY machinery; mitochondria; programmed cell death
Abbreviations: Clp, casenolytic proteases; PCD, programmed cell death; FITC–VAD–FMK, fluorescein isothiocyanate-valyl-alanyl-aspartyl-[O-methyl]-fluoromethyl-ketone; Ant, antennapedia internalization sequence; $\Delta\psi_m$ mitochondrial membrane potential; Z-GGL-AMC, benzyloxycarbonyl-glycyl-glycyl-leucyl-7-amido-4-methylcoumarin; TUNEL, terminal deoxynucleotidyl transferase dUTP nick end labeling
Received 13.5.11; revised 16.9.11; accepted 30.9.11; Edited by M Piacentini

Results

PfClpQ and PfClpY are expressed in the asexual blood-stage parasites and form a protein complex. We have earlier identified and characterized *P. falciparum* homolog of ClpQ protease (PfClpQ).[15] We have now identified *P. falciparum* ClpY orthologue (PfClpY) (See supporting information) (Figures 1a and b and Supplementary Figure S1). Real-time quantitative PCR analyses showed that transcription of *pfclpY* and *pfclpQ* start in trophozoite stages, with maximum transcript levels in late-trophozoite- and schizont-stage parasites (Supplementary Figure S2). Western blot analysis using anti-PfClpY antibodies with total parasite lysates detected PfClpY as a ~100 kDa protein in trophozoite and schizont stages (Figure 1c). In addition, a lower band of ~55 kDa was also detected that may represent the processed fragment of PfClpY. The western-blot analysis using anti-PfClpQ antibodies detected the pro-PfClpQ (~22 kDa) and mature-PfClpQ (~18 kDa) in trophozoite- and schizont- stage parasites with maximum expression in schizont stage. These results suggest that both PfClpQ and PfClpY are expressed in the blood-stage parasites in the late-trophozoite and schizont stages.

We next carried out co-immunoprecipitation studies to ascertain that the PfClpQ and PfClpY form a protein complex in the parasite. Western-blot analysis of immunoprecipitated complex showed that the PfClpQ gets co-immunoprecipitated with PfClpY from parasite lysate (Figure 1d). The PfClpQ was not detected in eluates from control reactions with pre-immune sera or with non-specific antibodies in place of anti-PfClpY antibodies. These experiments suggest that the ClpQ and ClpY are present in the same protein complex in the parasite; detailed *in vitro* and yeast two-hybrid assays were carried out, as described below, to assess if these two proteins interact directly to form the protein complex as in case of other organisms.[6–8]

PfClpY interacts with PfClpQ through its C terminus to form a protein complex. To ascertain the direct interaction of PfClpQ and PfClpY and to decipher role of C-terminal region of PfClpY in this interaction, we carried out different protein–protein binding assays using recombinant proteins, as well as by yeast-two-hybrid assays. In an *in vitro* solution-binding assay, PfClpQ formed a protein complex with PfClpY that was pulled down by anti-PfClpY antibodies (Figure 2a); however PfClpQ did not form a protein complex in control experiments where PfClpY was replaced with another recombinant protein, $PfMSP1_{19}$. Next, we also carried out *in vitro* solid-phase interaction studies using recombinant PfClpY and PfClpQ to ascertain their interaction. The PfClpQ

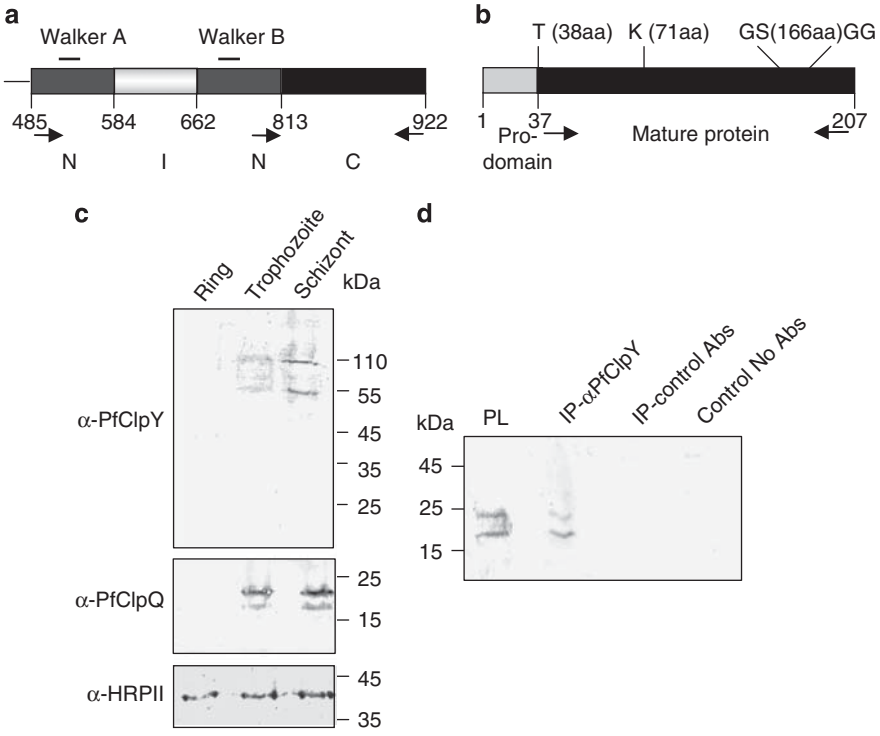

Figure 1 PfClpQ and PfClpY are expressed in the asexual-stage parasites and form a protein complex in the parasite. (**a**) Schematic domain structure of PfClpY (Gene ID PFI0355c) showing location of N, I and C domains, respective amino-acid positions and walker A and B domains are also indicated. (**b**) Schematic representation of structure of PfClpQ showing location of pro-domain and mature protease. The locations of conserved residues of active site triad are also marked. (**c**) Western blot analyses of total lysates of equal number of synchronized parasites at ring (8–10 h post invasion (hpi)), trophozoite (30–32 hpi) and schizont (42–45 hpi) stages with antibodies against the PfClpQ and PfClpY showing expression of both the proteins in trophozoite-schizont stages. Anti-histidine rich protein-II (HRPII) antibodies were used to probe a blot run in parallel to show equal loading in each well. (**d**) Co-immunoprecipitation of PfClpQ and PfClpY from parasite lysate using anti-PfClpY antibodies; PfClpQ protein was detected in the immunoprecipitated protein complex by western blot analysis. Immunoprecipitation reactions using non-specific antibodies or no antibodies were used as controls

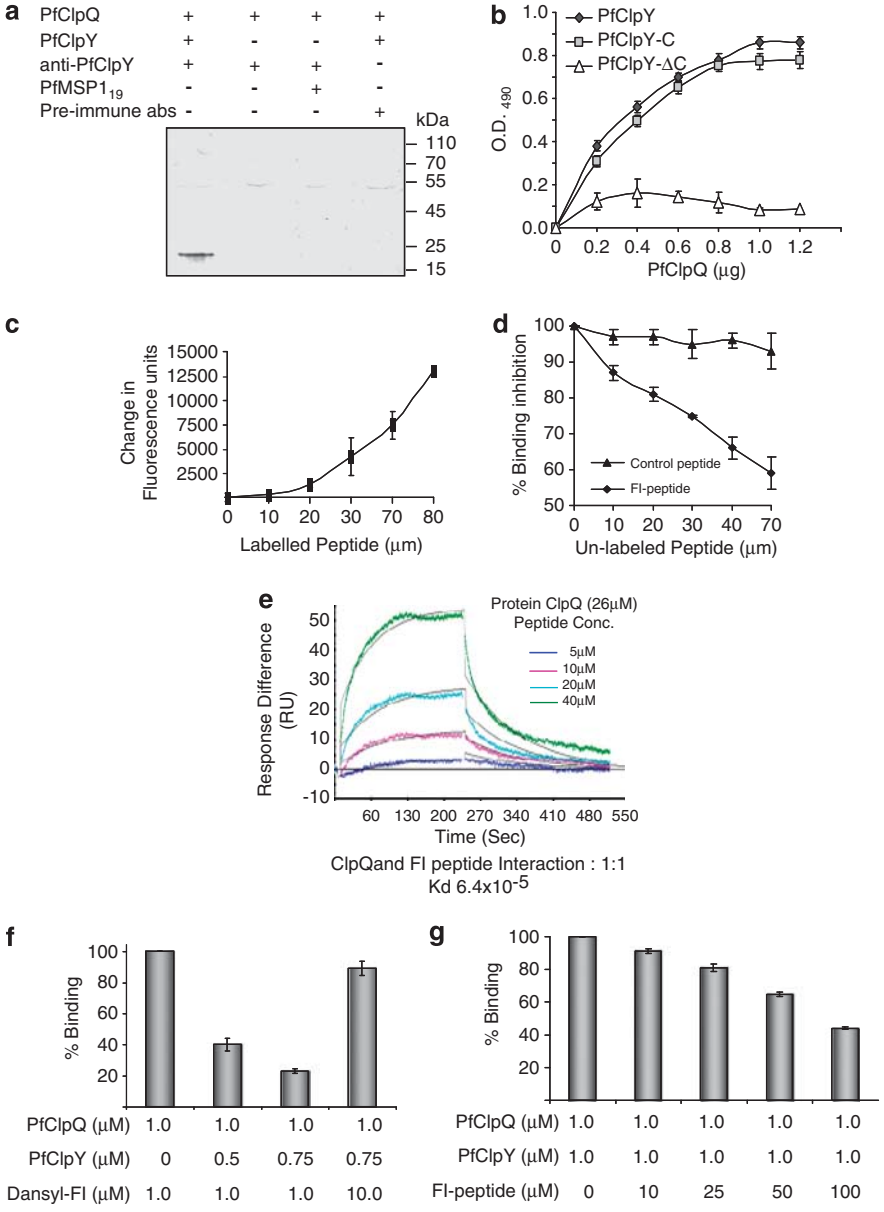

Figure 2 (**a** and **b**) Interaction of PfClpQ with PfClpY and its C-terminal fragments. (**a**) Solution-binding assays of PfClpQ and PfClpY recombinant proteins followed by *in vitro* pulldown of the protein complex using anti-PfClpY antibodies; PfClpQ protein was detected in the pulled down protein complex by western blot analysis. Control reactions were carried out in the absence of PfClpY protein or replaced with a non-specific protein (PfMSP-1_{19}); in another reaction the anti-ClpY antibodies were replaced with control antibodies (pre-immune). (**b**) *In vitro* solid-phase interaction of PfClpQ with increasing concentration of PfClpY and its C-terminal fragments; protein–protein interaction was estimated by ELISA using anti-PfClpY antibody. The PfClpY and PfClpY-C showed concentration-dependent interaction with PfClpQ, whereas PfClpY-ΔC showed no significant binding. (**c**–**e**) Interaction of synthetic peptide corresponding to C terminus of PfClpY (Fl-peptide) with PfClpQ protein. (**c**) A solution-binding assay of PfClpQ with Dansyl-labeled Fl-peptide (Dansyl-Fl), complex formation lead to change in fluorescence in the reaction. Fluorescence change (ΔF) was estimated using different concentration of the labeled peptide. The labeled peptide showed concentration-dependent binding with PfClpQ. (**d**) Inhibition of binding of Dansyl-Fl and PfClpQ in presence of increasing concentration of unlabeled Fl-peptide. Increasing concentration of unlabeled Fl-peptide reduced binding of Dansyl-Fl in a concentration-dependent manner. (**e**) Global fitting of the sensograms obtained by flowing increasing concentrations (5, 10, 20, 40 μM) of Fl-peptide for 4 mins on PfClpQ immobilized on the CM5 chip and dissociation for 4 min under similar flow conditions. Buffer alone was used as control that showed no responses to PfClpQ. (**f** and **g**) Fl-peptide and PfClpY shares the binding site on PfClpQ. (**f**) Percentage binding of Fl-peptide and PfClpQ in a solution-binding assay in absence or presence of increasing concentration of PfClpY. Presence of PfClpY reduced the binding of Fl-peptide and PfClpQ; a 10-fold increase in Fl-peptide concentration restored the binding with PfClpQ. (**g**) Percentage binding of PfClpQ and PfClpY in a ELISA-based assay in absence or presence of increasing concentration of Fl peptide

showed binding with the PfClpY in a concentration-dependent manner. Further, the C-terminal fragment of PfClpY, PfClpY-C, showed binding with PfClpQ in a similar manner. However, its truncated version, PfClpY-ΔC, showed poor binding with PfClpQ (Figure 2b). Results of yeast two-hybrid analyses also suggested that PfClpQ and PfClpY interact with each other and form a protein complex, this interaction is through C-terminal domain of PfClpY and a

stretch of residues in its C terminus has an important role in this interaction (see Supplementary information; Supplementary Figure S4; Supplementary Table S2).

C-terminal peptide of PfClpY (FI peptide) binds with PfClpQ and shares the binding site with PfClpY. To further study the role of C-terminal region of PfClpY in its interaction with PfClpQ, we used a 12-amino-acid-long synthetic peptide (FI-peptide) corresponding to the C terminus of PfClpY. Binding of PfClpQ with FI-peptide was studied by fluorescence spectroscopy using dansylated derivative of FI-peptide, Dansyl-FI. The labeled peptide showed binding with recombinant PfClpQ in a concentration-dependent manner (Figure 2c). To ascertain specificity of this interaction, the interaction of labeled peptide (Dansyl-FI) was competed with increasing concentrations of unlabeled FI-peptide. The unlabeled peptide was able to compete effectively with the labeled peptide and inhibited its binding with PfClpQ (Figure 2d); however, no inhibition was seen with a non-specific peptide.

A surface plasma resonance-based biomolecular-interaction analysis was carried out to quantitatively assess binding of ClpQ and FI-peptide. In this assay, the recombinant PfClpQ was used as ligand and FI-peptide was used as analyte. The assay channel showed typical association and dissociation curves as compared with the control cells, which show little fluctuation due to solvent (Figure 2e). However, no difference in response units was detected when FI-peptide was injected in either blank flow cells or flow cells coated with a non-specific *P. falciparum* recombinant protein (MSP-1_{19}). Similarly, no response was observed when a scrambled-FI-peptide was flowed over immobilized PfClpQ. Therefore, BIACORE analysis shows specific binding of PfClpQ with the C-terminal peptide, FI. The calculated binding constant, K_d, for the ClpQ and FI-peptide interaction was estimated to be 62.4 μM with rate constants, k_a, of 157/M s, and dissociation rate constants, k_d, of 9.76×10^{-3}/s (the chi-square value for the fit is 2.39). However, the binding constant and the dissociation constant of PfClpQ–FI interaction suggest that the interaction has low binding affinity. A low signal/background ratio in the danyslated-peptide assays and low binding-peptide affinity may be responsible for high peptide concentration required in the interaction studies (Figure 2).

To ascertain that the FI-peptide and PfClpY share the same binding site on PfClpQ, solution-binding assays of Dansyl-FI-peptide and PfClpQ were carried out in presence of PfClpY. As shown in Figure 2f, presence of PfClpY in the assay reduced binding of FI-peptide with PfClpQ. Level of inhibition was a function of PfClpY concentration at a fixed concentration of FI-peptide. However, when FI-peptide concentration was increased, it was able to overcome this antagonism of PfClpY and restored it's binding with PfClpQ. These results suggest that there is competition between FI-peptide and PfClpY to bind with PfClpQ, and thus the FI-peptide shares the PfClpQ-binding site with PfClpY protein. Further, we also assessed the inhibition of PfClpY–PfClpQ binding in the ELISA experiment by FI-peptide. Interaction of PfClpQ and PfClpY was inhibited in presence of FI-peptide. The level of inhibition was a function of FI-peptide concentration (Figure 2g). However, as discussed above, a relatively high concentration of FI-peptide is required to interfere with PfClpQ–PfClpY interaction.

Effect of FI-peptide treatment on parasite growth. We next investigated effect of FI-peptide on parasite growth and development *in vitro*. To facilitate uptake of the peptide, a 16-aa sequence of Antennapedia (Ant) homeoprotein was coupled to the amino terminus of FI-peptide (Ant-FI) (Supplementary Figure S5). The Antennapedia internalization sequence has been known to facilitate uptake of peptides into *P. falciparum*.[17,18] Treatment of parasite cultures with Ant-FI-peptide inhibited parasite growth in a dose dependent manner (Figure 3a). At 50 μM concentration Ant-FI-peptide showed $\sim$50% growth inhibition, and at 100 μM it showed 90–95% growth inhibition (Figure 3a) as compared with control. The effector concentration for half maximum response (EC_{50}) value was $\sim$50 μM. No significant growth inhibition was observed in culture treated with Ant-Scr control peptide (Figure 3a).

We also assessed any eventual recovery of FI-peptide treated culture after removing the peptide at different time points. Removal of the peptide at 1–3 h after treatment resulted in almost complete reversal of growth inhibition and parasite cultures were able to recover; when peptide was removed at 4 h time point there was $<$20% growth inhibition suggesting that about 80% of parasites were able to recover the growth. However, when peptide was removed at 6 h after treatment, a large percentage of parasite ($>$40%) population was not able to recover (Supplementary Figure S6). Similarly lower percentage population of parasite was able to recover the growth when the peptide was removed at 8 or 16 h after treatment (Supplementary Figure S6).

Disruption of PfClpQY activity by FI-peptide disrupts the intra-erythrocytic parasite cycle. To study the effect of Ant-FI-peptide on parasite development and morphology, synchronized parasite cultures at early-trophozoite stages were treated with Ant-FI-peptide at 50 μM or 90 μM concentrations ($\sim EC_{50}$ and $\sim EC_{90}$ respectively). In control sets, parasites developed from early-trophozoites to late-trophozoites in 6–8 h after treatment and subsequently into mature schizonts within 12–16 h after treatment. The merozoites released from these schizonts invaded new RBCs and developed into ring-stage parasites 24–30 h after treatment (Figure 3b). However, parasite treated with Ant-FI-peptide showed abnormal developmental morphology; in addition, these parasites were not able to develop into schizonts. A large percentage of parasites in cultures treated with Ant-FI-peptide showed condensed cytosol, darkly stained nucleus and abnormal shape of plasma membrane within 8–10 h after treatment (Figure 3c); later the parasite cytosol became completely condensed and parasites appeared as densely stained structures (Figure 3c). The percentage of parasites with these 'crisis form morphology' increased with the incubation time and peptide concentration. At 50 μM, about 55% of parasites showed crisis form morphology within 10–15 h after treatment, whereas at 90 μM peptide concentration, almost all parasites showed abnormal morphology and turned into condensed round densely stained pycnotic

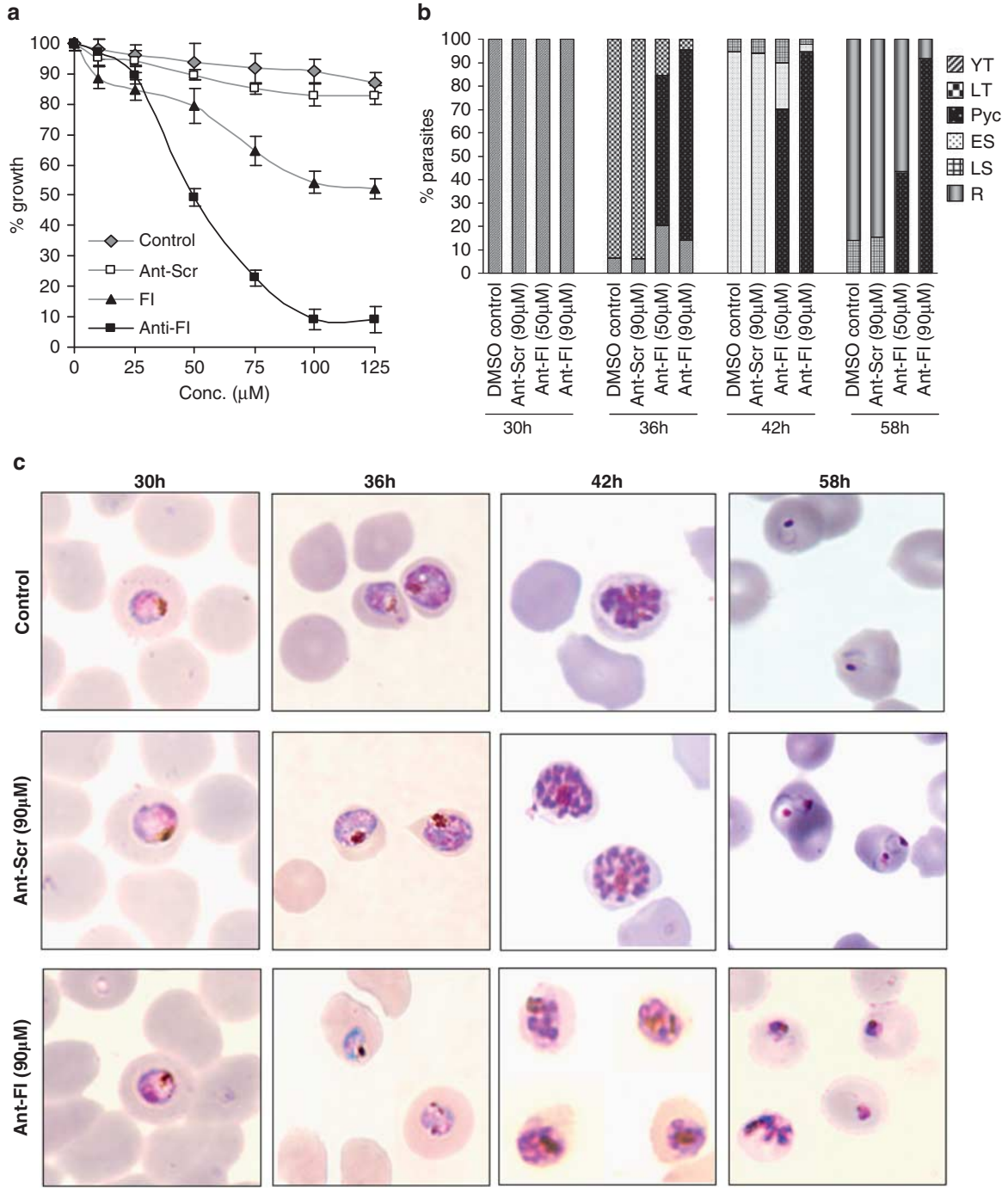

Figure 3 Effect of FI-peptide treatment on growth and development of *P. falciparum*. (**a**) Tightly synchronized early-trophozoite-stage parasite cultures (~ 30 hpi) were treated with different concentration of FI-peptide, Ant-FI peptide, Ant-scrambled peptide and solvent alone, percentage parasite growth was estimated by formation of new ring-stage parasites as compared with untreated culture. (**b**) Effect of Ant-FI-peptide treatment (at 50 and 90 μM) on parasite stage composition at different time points (30–58 hpi). The percentage of parasites at young trophozoite (YT), late trophozoite (LT), early schizont (ES), late schizont (LS), ring stage (R), and stressed pycnotic forms (Pyc) are indicated. (**c**) Effect of Anti-FI-peptide treatment (at 90 μM) on parasite morphology at different time points (30–58 hpi)

forms within 10–15 h after treatment (Figure 3c). These parasites remained as pycnotic forms in the culture and did not show any vacuolated structure. These parasites were not able to develop into schizonts or form any merozoites (Figure 3b).

FI-peptide treatment disrupts mitochondria membrane potential ($\Delta\psi_m$). The morphological phenotypes induced by FI-peptide treatment of parasites were reminiscent of apoptosis phenotype. Therefore, we examined the treated parasites for cellular features associated with the apoptosis.

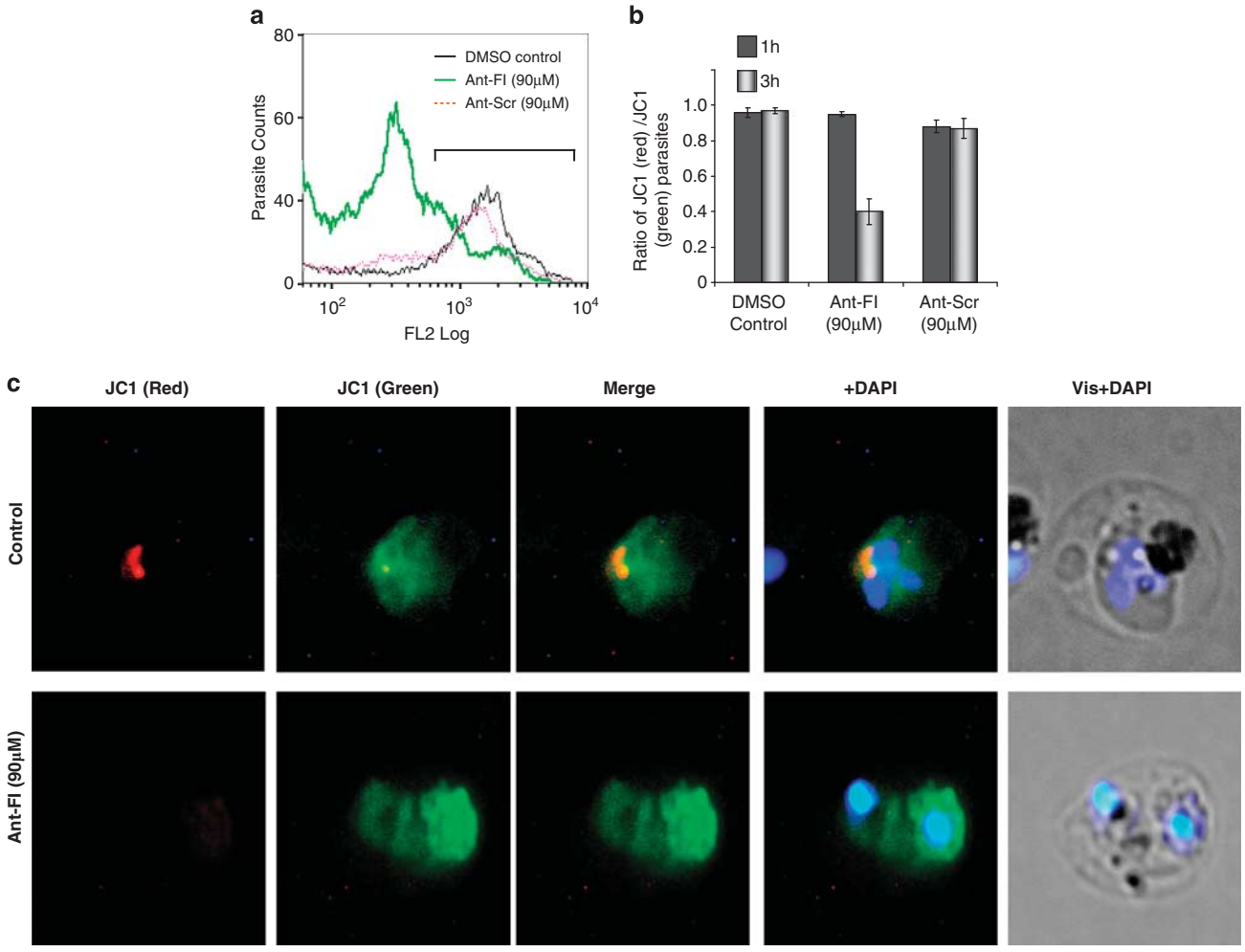

Figure 4 *In situ* mitochondrial membrane potential of *P. falciparum* parasite after treatment with Ant-FI-peptide as estimated by JC-1 staining. (**a**) Flow-cytometry histogram showing reduction in JC-1 red staining in the parasite population treated with Ant-FI-peptide as compared with parasites treated with scrambled peptide or solvent alone. (**b**) Graph showing ratio of JC-1 (red)/JC-1 (green) parasite population after treatment with Ant-FI, Ant-Scrambled (Ant-Scr) or solvent alone. (**c**) Fluorescent microscopic images of JC-1-stained parasite showing accumulation of aggregated JC-1 (red staining) in the mitochondria and monomeric JC-1 (green staining) in the cytosol. Treatment of Ant-FI-peptide caused loss of membrane potential, which reduced red staining in the mitochondria of the parasite. The parasite nuclei were stained with DAPI (blue) and parasites were visualized by fluorescence microscope

Given that the mitochondria is a key component of onset of apoptosis and ClpQY machinery is functional in the parasite mitochondria, we first studied the effect of Ant-FI-peptide treatment on mitochondria membrane potential by JC-1 dye staining. In the control set, the parasites showed JC-1-red staining that represents JC-1 aggregation in the mitochondria, suggesting presence of functional mitochondria (Figure 4a). The ratio of parasite population with mitochondrial red and cytosolic green staining in the control set was found to be ~1.0 (Figure 4b). Parasite treated with Ant-FI-peptide at ~EC_{90} showed a significant decrease in JC-1 red staining after 3 h (Figure 4a) leading to significant decline in the ratio of JC-1 red- and green-stained population to ~0.4 (Figure 4b, Supplementary Figure S7). Fluorescence microscopy also showed loss of JC-1 red staining in the mitochondria of the treated parasites (Figure 4c). These results clearly show loss of mitochondria membrane potential ($\Delta\psi_m$) in the parasite by FI-peptide treatment. No or little effect was seen at 1 h after treatment of the parasites as evident from JC-1 red/green ratio. Control parasite treated with solvent alone or with Ant-scrambled peptide showed no significant change in the membrane potential (Figures 4a and b).

Loss of $\Delta\psi_m$ in FI-peptide treated parasites activates caspase-like proteases and leads to apoptosis-like cell death in parasite. We next assessed if loss of $\Delta\psi_m$ leads to activation of any caspase-like cysteine protease activity in the parasite. Synchronized parasite cultures were treated with peptide or solvent alone, and analyzed at different time points for staining with CaspACE (FITC–VAD–FMK), a cell permeable and fluorescent tagged *in situ* marker that binds with activated caspase-like proteases. In solvent control sets, a basal level of staining was detected in 5–10% of the parasites. The Ant-FI-peptide (90 μM) treated parasite showed activation of caspase-like protease activity within 4 h of treatment; the percentage of cell showing fluorescent

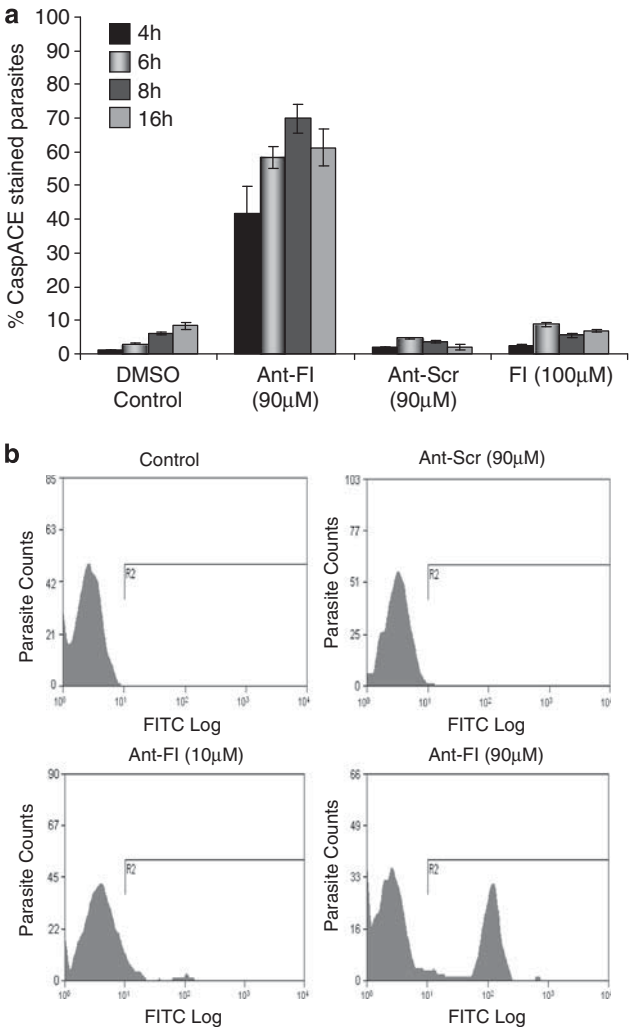

Figure 5 Activation of CaspACE–VAD–FMK binding cysteine proteases in *P. falciparum* parasite. (**a**) Graph showing percentage of CaspACE-tagged parasites in the cultures at different time points (4, 6, 8, and 16 h) after treatment with peptides Ant-FI, Ant-Scrambled (Ant-Scr) or solvent alone. (**b**) Flow cytometry histogram showing population of CaspACE-tagged parasites in cultures 4 h after Ant-FI treatment as compared with controls

labeling increased for 4–12 h after treatment reaching to a maximum of ~70% of parasites showing CaspACE staining (Figures 5a and b and Supplementary Figure S8). However, at time point earlier than 4 h there was no significant increase in CaspACE-stained parasite population in the treated cultures as compared with the control, suggesting that activation of VAD–FMK-binding proteases occur ~4 h after the treatment. At 16 h after treatment, there was some decrease in the number of stained parasites, which may be due to increase in number of parasites in pycnotic crisis form (Figures 5a and b and Supplementary Figure S8).

Further, we also analyzed the DNA fragmentation in the parasites by using the TUNEL assay. The Ant-FI-peptide-treated parasites showed TUNEL staining that overlapped with the DAPI staining, (Figures 6a and b) suggesting fragmentation of the nuclear DNA. The percentage of parasite showing TUNEL staining increased as a function of peptide concentration and time after treatment. Parasites treated with peptide at ~EC_{50} (50 μM) showed TUNEL-positive cells 4 h after the treatment with maximum percentage of TUNEL-positive parasites ~50% at 16 h after treatment. Whereas cultures treated with peptide at ~EC_{90} (90 μM) showed almost all the parasites (~90%) with TUNEL staining at 16 h after treatment (Figure 6a). Control parasite treated with DMSO alone and parasite treated with Ant-scrambled peptide did not show any TUNEL staining in the parallel assay.

Discussion

The ClpQY protease machinery consists of the ClpQ protease and an AAA + chaperon ClpY, which together form multimeric protein complex, presenting structural and functional analogies with the eukaryotic 26S proteasome. In the present study, we have identified full ClpQY system in the malaria parasite. Our results show that the ClpQ and ClpY protein in *P. falciparum* are part of a protein complex as shown in prokaryotes.[6–8] We have earlier carried out homology modeling and molecular docking studies of ClpQY protein complex, these studies combined with computational alanine scanning suggested mechanism of interaction between PfClpQ and PfClpY subunits through the C-terminal residues of PfClpY in the loop region.[19] To ascertain that the PfClpQ and PfClpY interact directly to form a protein complex, we carried out detailed *in vitro* and cell-based protein–protein interaction studies. Our results show that the PfClpQ and PfClpY interact with each other; the C-terminal region of PfClpY representing the C-domain (PfClpY-C) is involved in its interaction with PfClpQ and a short stretch of amino acids in the C terminus of PfClpY has a key role in this interaction. These results corroborated with our *in silico* interaction studies of the PfClpQY protein complex.[19] With a view to understand the functional role of ClpQY machinery in the parasite, we identified a peptide-based inhibitor that could be utilized to disrupt the interaction of PfClpQ and PfClpY, and hence inhibit function of ClpQY machinery in parasite. Small peptide-based antagonists that are copy of natural motifs involved in interactions of cognate proteins are being developed to disrupt high-affinity protein interactions and modulate target-protein machineries in the cells.[20–22] We assessed potential of a synthetic peptide (FI-peptide), corresponding to the short stretch at the C terminus of PfClpY, to bind with PfClpQ. The FI-peptide showed specific binding with PfClpQ; competition-binding assays showed that PfClpY and FI-peptide share the same binding site on PfClpQ; further, the FI-peptide also antagonizes PfClpQ and PfClpY interaction. These results suggest that FI-peptide can be used to disrupt the ClpQY functioning in parasites and study functional significance of this protease machinery. Recently, small peptides and peptide-based inhibitors have been successfully used to block function of different proteases and inhibit malaria parasite growth.[17,18,23] The FI-peptide treatment caused severe inhibition of parasite growth; further, development of treated parasites was effected and these parasites were not able to develop into mature schizonts. However, micromolar concentrations of FI-peptide are needed to exert the effect on parasite growth; this could be due to slow uptake of peptides by parasites. Indeed, only high

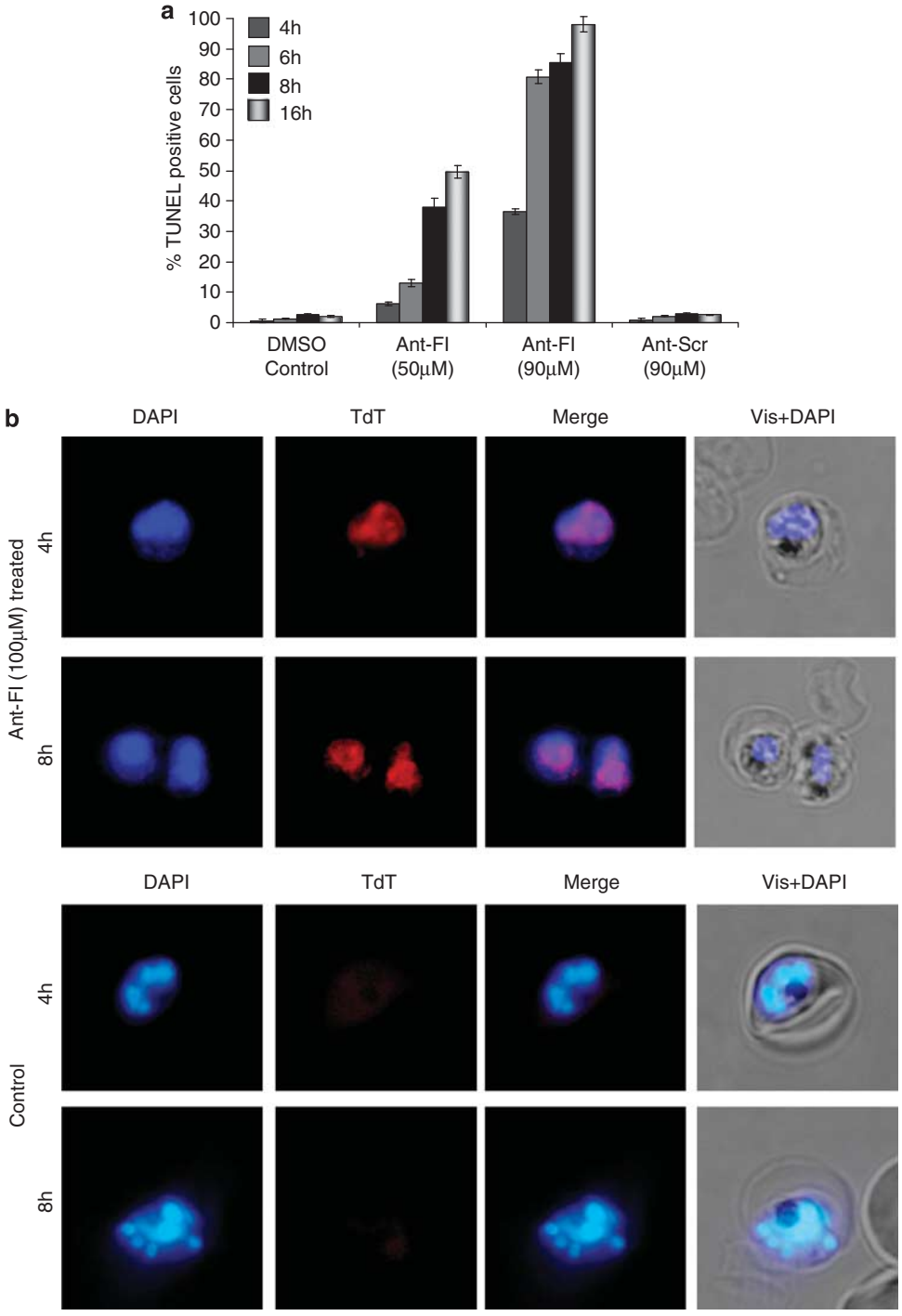

Figure 6 DNA fragmentation in *P. falciparum* parasites as assessed by TUNEL staining. (**a**) Graph showing percentage of TUNEL-positive parasites in the cultures at different time points (4,6,8 and 16 h) after treatment with peptides Ant-FI (50 and 90 μM), Ant-scrambled (Ant-Scr, 90 μM) or solvent alone. (**b**) Fluorescent microscopic images of TUNEL-positive parasites (TdT red staining) in treated cultures as compared with controls. The parasite nuclei were stained with DAPI (blue) and parasites were visualized by fluorescence microscope

micromolar concentrations of peptide inhibitors are shown to affect parasite growth in earlier studies.[17,18]

The ClpQ protease was recently localized in the matrix of the mitochondria in *P. falciparum*;[23] similarly, ClpQ orthologue was also localized in mitochondria of *Trypanosoma brucei*.[24] Parasite mitochondrion has an important role in critical biosynthetic processes, including iron–sulfur cluster biosynthesis, heme biosynthesis and ubiquinone biosynthesis.[25] As ClpQY is the only protease machinery localized in the mitochondria, it may be having an important role in the

mitochondrial functioning in the apicomplexan parasites. Indeed, knocking down of ClpQ orthologue in *T. brucei* lead to reduced growth of parasites.[24]

The *Plasmodium* mitochondrion has a linear ~6 kb-long genome that encodes three proteins, Cox1, CytB and Cox3, as well as a number of rRNA subunits.[26,27] In addition, >350 nuclear-encoded proteins are targeted to the parasite mitochondrion.[28] These proteins have roles in different metabolic pathways in the mitochondrion. Deregulation of metabolic pathways in mitochondria and loss of mitochondrial membrane potential is usually lethal for eukaryotic cells. Inhibition of ATP-dependent Lon protease in mitochondria of eukaryotic cells caused accumulation of aggregated proteins, which subsequently lead to apoptosis of cells.[29] The ClpQY system in parasite mitochondria might have an important regulatory role for the parasite. Indeed, silencing of ClpQ in *T. brucei* showed loss of control of replication of minicircle DNA in the mitochondria leading to reduced parasite growth.[24] *Plasmodium* mitochondrion does not possess minicircle DNA, and the ClpQY machinery may be involved in regulation of proteins involved in other metabolic pathways. Our results with parasite growth-inhibition assay using FI-peptide suggest that the ClpQY protease machinery has an important functional role in *Plasmodium* mitochondria; any interference in its activity could destabilize the mitochondrial functioning. Inhibition of ClpQY protease machinery using interfering FI-peptide caused significant loss of mitochondrial membrane potential. This effect was combined with morphological phenotypes of the parasites that are reminiscent of the apoptosis-like phenotype, including condensation of cytosol and darkly stained nucleus. Induction of apoptosis-like features in asexual stage *P. falciparum* parasites is shown after chloroquine treatment, which include cellular characteristics, such as loss of mitochondrial membrane potential ($\Delta\psi_m$), activation of caspase-like cytseine proteases and nuclear DNA fragmentation.[30,31] In the present study, disruption of ClpQY machinery also resulted in loss of $\Delta\psi_m$, which subsequently lead to increased number of CaspACE-tagged parasites and DNA fragmentation of the parasites. These results suggest that inhibition of the ClpQY machinery caused deregulation of mitochondrial growth and functioning. Dysfunctioning of mitochondria in turn acts as an intrinsic signal in the parasite, which initiates a cascade of reactions leading to apoptosis-like cell death. We also assessed any eventual recovery of the FI-peptide-treated culture after removing the peptide at different time points; the FI-peptide treatment can be reversed in early stage (1–4 h), however longer treatment induces changes in the parasite with point of no return.

We further show that activation of VAD–FMK-binding proteases and DNA fragmentation follow after the loss of $\Delta\psi_m$ in the parasite; loss in $\Delta\psi_m$ started at 2–3 h after treatment whereas caspase like-activity and DNA fragmentation were observed at 4–6 h after treatment. The *P. falciparum* genome does not contain any classical caspase-like protein. Caspase-like activity is also described during apoptosis in other organisms that lack classical caspases.[32–34] Although *P. falciparum* genome also harbors two metacaspase-like proteases that are closely related to eukaryotic caspases, it is still not clear if these proteases are directly involved in apoptosis-like process in parasites. Our results show that VAD–FMK-binding proteases get activated after loss of $\Delta\psi_m$ and dysfunctioning of the mitochondria. The identity of VAD–FMK-binding proteases, exact role of these proteases, specific target substrates and complex cascade of induction/activation during apoptosis in parasites remains to be elucidated.

Overall, we have identified the complete ClpQY machinery in *P. falciparum* and show that the ClpQY machinery is important for maintenance of functional mitochondria in parasites. Our results suggest that deregulation of parasite mitochondria triggers a cascade of reactions that leads to apoptosis-like cell death in the parasite.

Materials and Methods

Parasite culture, and growth inhibition assays. *P. falciparum* strain 3D7 was cultured with human erythrocytes (4% hematocrit) in RPMI media (Invitrogen, Eugene, OR, USA) supplemented with 10% O+ human serum using a protocol described previously.[35] Cultures were synchronized by repeated sorbitol treatment, following Lambros and Vanderberg.[36] The amino-acid sequences of all the peptides used in the study are given in Supplementary Table S1. Assays for growth inhibition by different peptides were performed as previously described.[17] Briefly, tightly synchronized *P. falciparum* 3D7 parasites at early-trophozoite stage were cultured in 96-well plates in which hematocrit and parasitemia were adjusted to 4.0% and 0.8%, respectively. Purified peptides were added to the parasite cultures to variable final concentrations (1.0–125 μM). Control wells were treated with solvent alone. Each assay was performed in triplicate and the experiment was repeated at least twice. The cultures were incubated for 24 h, smears were made from each well at different time points and stained with Giemsa. To assess growth of the parasite, numbers of new ring-stage parasites formed were determined per 5000 RBCs, percentage parasitemia was calculated and percentage growth was calculated as compared with the parasitemia in solvent controls. To assess any recovery of the treated culture after peptide removal, the parasite cultures were treated with the peptide at ~EC_{50} as described above, subsequently the cultures were washed with RPMI at different time points after treatment (1–16 h) to remove the peptide. Inhibition of parasite growth was assessed as described above and compared with unwashed controls.

Isolation of DNA, total RNA and quantitative RT-PCR. The genomic DNA was isolated from *in vitro* culture of *P. falciparum* following a standard protocol.[37] Total RNAs were isolated from synchronized *P. falciparum* 3D7 parasite cultures using mini-RNA isolation kit (Qiagen, Hilden, Germany). An aliquot of 50 ng of total RNA was used to synthesize cDNA using cDNA synthesis kit (Invitrogen) following manufacturer's recommendations. Gene-specific primers were designed using Beacon Designer4.0 software (Premier Biosoft, Palo Alto, CA, USA), for the genes *pfclpY* (416A, 5′-TTATATCCTCATGAGATTGTGGAATATTTG-3′ and 461-2A, 5′-TTACCATGAAATCCAACTTCTGTAAAC-3′), *eba175* (EBA175RTF: 5′-AATTTCTGTAAAATATTGTGACCATATG-3′ and EBA175RTR: 5′-GATACTGCACAACACAGATTTCTTG-3′) and *falcipain 2* (Fal2F 5′-GCTTGTAGGTTTTGGTATGAAAGAA-3′ and Fal2 R 5′-AGATAGGTCCCTTTTTAAAATACTATTGAC-3′);[38] 18S rRNA control primers (18SF 5′-GCTGACTACGTCCCTGCCC-3′; 18SR 5′-ACAATTCATCATATCTTTCAATCGGTA-3′) were used following.[39] Quantitative real-time PCR were carried out in triplicate using the iCycler version 3.0 (Bio-Rad); each reaction was containing equal amount of cDNA, 100 ng of each gene-specific primers and 1 × SYBR Green PCR mix (Bio-Rad, Hercules, CA, USA). Threshold cycle (Ct) values were calculated by using iCycler software. Standard curves for each gene were obtained by using different dilutions of wild-type gDNA (100–1 ng) as template, and these standard curves were used to determine genome equivalents of Ct values for every gene and 18S rRNA in each RNA sample.[39] Genome equivalents of each gene were normalized using that of 18S rRNA for all RNA samples.

Expression and purification of recombinant proteins (PfClpQ, PfClpY and C-terminal fragments of PfClpY) and ATPase assay. Expression and purification of recombinant protein corresponding to mature region of PfClpQ (38–170 aa) was carried out as described earlier.[14] The threonine protease activity of purified-PfClpQ protein was assessed using fluorogenic-peptide substrate Z-GGL-AMC as described earlier.[14] A large fragment of PfClpY (485–922 aa) harboring N-, I- and C-domains, was amplified from total

cDNA of the parasite by PCR using primers 563A, 5′-GGC*GGATCC*CTTATATCC TCATGAGATTGTGG-3′ and 415A, 5′-CCG*AAGCTTCTCGAG*TTATATGATATATT TATTATAGTCGTATTGC-3′. The amplified PCR product was digested with *BamH*I and *Hin*dIII and cloned into *BamH*I and *Hin*dIII sites of pET28b vector (Novagen, Merck Biosciences Ltd., Darmstadt, Germany). The recombinant plasmid pET28b-PfClpY was transformed into *Escherichia coli* expression cells BL21(DE3) (Novagen) for expression of recombinant protein with N-terminal histidine tag. These cells were grown in Luria broth containing ampicillin (100 μg/ml) at 37 °C to an $OD_{600\,nm}$ of 0.5–0.6 and expression of the recombinant protein was induced with isopropyl-β-thioglactopyranoside (IPTG) at a final concentration of 1.0 mM. The cultures were then allowed to grow for an additional 2 h at 37 °C with shaking and the *E. coli* cells were harvested by centrifugation. The cell pellet was suspended in lysis buffer (20 mM Tris pH 8.0, 250 mM NaCl, 5 mM benzamidine-HCl, 0.05% Tween 20), lysed by sonication (Torebeo Ultrasonic Processor36800, Cole Parmer, Vernon Hills, IL, USA) and centrifuged at 12 000 r.p.m. for 20 min at 4 °C. The inclusion-bodies pellet obtained was lysed in lysis buffer (10 mM Tris-HCl, 100 mM NaCl, 6 M Gu-HCl, 10 mM Imidazole, pH 8.0) and the recombinant protein was purified by affinity chromatography using Ni-NTA resin. The protein was refolded by rapid dilution in a buffer containing 50 mM Tris-HCl buffer pH 7.4, 1 mM EDTA, 1 M urea, 2 mM reduced glutathione, 0.2 mM oxidized glutathione, 0.1 mM PMSF and 0.5 M L-Arginine, keeping a final protein concentration of <0.8 mg/ml. Subsequently, the sample was dialyzed against Tris-HCl buffer (pH 7.4) containing 20 mM NaCl, and the recombinant protein was purified by an-ion exchange chromatography using Q-Sepharose resin. Fractions containing pure PfClpY protein were pooled and concentrated.

A C-terminal fragment of PfClpY (725–922 aa) harboring the C-domains, was amplified from total cDNA of the parasite by PCR using primers 601-2A, 5′-GGC GCCATGGAAGAAGGAATTGTTTTTATAG-3′ and 570A, 5′-GCCGGATCCTTATA TGATATATTTTTTTAAGTCGTATTGC-3′. The amplified fragment was cloned into *Nco*I and *BamH*I sites of pET32b vector (Novagen) to give pET32-PfClpY-C construct. A similar PfClpY fragment with 12-residue deletion at the C terminus (725–910 aa; PfClpY-ΔC) was amplified using primers 601-2A, and 571A, 5′-GCC GGATCCTTAAATAAAACCTTCCAGCG-3′, the amplified fragment was cloned in pET32b vector to give pET32-PfClpY-ΔC. The recombinant PfClpY-C and PfClpPY-ΔC proteins were expressed in *E. coli* cells harboring respective plasmid construct. The recombinant proteins were purified from cytosolic fractions by affinity chromatography as described above using a column of Ni-NTA resin.

The hydrolysis of ATP by PfClpY was analyzed by pyrophosphate (^{32}P)-release assay using γ^{32}P-ATP. The reaction mixture consisting of labeled γ^{32}P-ATP (9 μCi) and unlabeled ATP (1 mM), 1–10 μg of recombinant PfClpY protein in 20 mM Tris-HCl (pH 8.0) buffer containing 8 mM DTT, 1.0 mM $MgCl_2$ and 10 mM KCl was incubated at 37 °C for 2 h followed by thin-layer chromatography. The chromatography plate was air dried and exposed to the X-ray film.

Generation of polyclonal anti-sera and western immunoblotting. To generate polyclonal anti-sera against PfClpY, female BALB/c mice were immunized (on day 0) with the purified recombinant protein (25 μg) formulated in complete Freund's adjuvant (Sigma, St. Louis, MO, USA). The mice were administered two booster doses (day 14 and 28) of the proteins formulated in Freund's incomplete adjuvant. The mice serum was collected 10 days after the second boost.

For western blot analyses, parasites were isolated from tightly synchronized cultures at different developmental stages by lyses of infected erythrocyte with 0.15% saponin. Parasite pellets were washed with PBS, suspended in Laemmli buffer, boiled, centrifuged, and the supernatant obtained was separated on 12% SDS-PAGE. The fractionated proteins were transferred from gel onto the nitrocellulose membrane (Amersham, Piscataway, NJ, USA) and blocked in blocking buffer (1 $\times$ PBS, 0.1% Tween-20, 5% milk powder) for 2 h. The blot was washed and incubated for 1 h with primary antibody (mouse anti-PfClpY (1 : 500); rabbit anti-PfClpQ (1 : 1000); rabbit anti-HRPII (1 : 2000)) diluted in dilution buffer (1 $\times$ PBS, 0.1% Tween-20, and 1% milk powder). Later, the blot was washed and incubated for 1 h with appropriate secondary antibody (anti-rabbit or anti-mouse, 1 : 2000) conjugated to HRP, diluted in dilution buffer. Bands were visualized by using ECL detection kit (Amersham).

***In vitro* binding assays for protein–protein and protein–peptide interactions.** Protein–protein interaction was assessed by solution binding of the two proteins followed by *in vitro* pulldown of the protein complex. Briefly, anti-PfClpY antibodies were allowed to bind with protein-A sepharose beads in 20 mM Tris pH 7.4, NaCl 150 mM (TBS) for 30 min at 4 °C with gentle agitation, the beads were then blocked with 5% BSA in TBS. Recombinant ClpY and ClpQ were allowed to bind with each other at 4 °C for 2 h (final concentration in the reaction 2 μg/ml of each) in the binding buffer. The mixture was then incubated (4 °C for 2 h) with protein A Sepharose beads having immobilized-anti-ClpY antibodies, to pull down the complex. After extensive washing with TBS-T (TBS containing 0.1% Triton- X 100) the beads were boiled in SDS-PAGE buffer and centrifuged. The supernatant was separated on SDS-PAGE, transferred to nitrocellulose and probed with anti-PfClpQ antibodies. In control reactions, the ClpY protein was either absent or replaced with a non-specific *P. falciparum* recombinant protein ($MSP\text{-}1_{19}$); in another control the anti-ClpY antibodies were replaced with control antibodies (pre-immune).

In vitro protein–protein interactions were also studied in an ELISA-based assay. Briefly, wells of Maxi-Sorp micro-titer plates (Nunc International, Nunc, Langenselbold, Germany) were adsorbed with recombinant PfClpY (100 ng in each well) at 4 °C. The wells were washed thrice with 1 $\times$ PBS containing 0.05% Tween-20 (PBS-T) and blocked with 1% BSA in 1 $\times$ PBS for 2 h. Purified recombinant ClpQ in varying concentrations (20–200 ng) was added to the ClpY-coated wells and incubated for 2 h at room temperature. Plates were then washed five times with PBS-T followed by sequential incubation with purified anti-ClpQ antibody (dilution 1 : 2000) and goat anti-mouse horse radish peroxidase (HRP)-labeled secondary antibody (dilution 1 : 3000). After repeated washing, the enzyme reactions were developed with 50 μl of *o*-phenylenediamine dihydrochloride-H_2O_2 in a citrate phosphate buffer (pH 5.0), the reactions were stopped with 25 μl of 2N H_2SO_4 and OD_{490} was measured using a 96-well micro-plate reader (Genios Pro; Tecan Instruments, Tecan, Männedorf, Switzerland).

Solution-binding assays were carried out to study interaction of ClpQ protein and peptides following Ramachandran *et al.*[40] The dansylated Fl-peptide (Dansyl-FIKQYDLKKYII) was added to varying final concentration (10–100 μM) in wells of a flat-bottom micro-titer plate containing 200 μl protein ClpQ (monomeric concentration of 13 μM) in 20 mM Tris, 300 mM NaCl. The fluorescence spectra from each well were recorded at emission and excitation wavelengths of 335 and 533 nm, respectively, using Fluo-Star micro-plate reader (BMG Technologies, BMG LABTECH, Ortenberg, Germany). Enhancement in fluorescence values (ΔF_{533}) were calculated after subtracting values from respective control wells where the dansylated peptide was added only to the buffer. For competition assay between dansylated and unlabeled Fl peptide, increasing concentrations (10–70 μM) of unlabeled peptide (FIKQYDLKKYII) were added to the wells containing ClpQ and 80 μM of dansylated peptide for the same assay. To assess the competition between Fl-peptide and ClpY for binding with recombinant ClpQ, the solution-binding assays were carried out in the same way using dansylated Fl-peptide in presence of varied concentrations of ClpY protein.

Surface-plasmon resonance analysis. Real-time interactions of PfClpQ with Fl-peptide (FIKQYDLKKYII) were analyzed by surface plasmon resonance studies under flow condition using Biacore 2000 instrument. The carboxymethylated-dextran surfaces of Biacore CM5 sensor chips were activated by injection of 1 : 1 mixture of *N*-hydroxysuccinimide (NHS) (Biacore AB, Biacore, Uppsala, Sweden) and 1-ethyl-3-(3-dimethylaminopropyl)-carbodiimide hydrochloride (EDC) (Biacore AB) for 7 min at a flow rate of 10 μl/min. Recombinant PfClpQ (10 μg/ml in 10 mM sodium acetate buffer, pH 4.5) was injected over the activated surface of a sensor chip flow cell at a flow rate of 10 μl/min so as to achieve an immobilization equivalent to 500 RU. A non-specific recombinant protein was immobilized on surface of another sensor chip flow cell in similar way and was used as a negative control. A third sensor chip flow cell was blocked by injection of ethanolamine (Biacore AB) at a flow rate of 10 μl/min for 5 min and was used as blank. Kinetic-binding analysis for interaction of PfClpQ was carried out by injecting the Fl-peptide at different concentrations (5, 10, 20, 40 μM) in independent experiments. The peptide or recombinant proteins were injected for 4 min at a flow rate of 30 μl/min with the running buffer (10 mM HEPES, pH 7.4, 150 mM NaCl, 3 mM EDTA and 0.005% P20 surfactant); the dissociation was monitored for 240 seconds with the running buffer at the same flow rate. To correct for refractive index changes caused by running buffer and instrument noise, running buffer was injected at a flow rate of 30 μl/min in the blank flow cells and the observed response difference was subtracted from the experimental data. The flow rate of the peptide and the recombinant proteins was varied from 10 to 75 μl/min in order to assess whether the binding interactions were limited by mass transfer. A non-specific peptide (Ant peptide) was used in the control experiments. The experimental surface was regenerated by injecting regeneration solution (1 M ethanolamine) at a

flow rate of 30 μl/min for 1 min. The binding constant, Kd, was calculated as kd1/ka1 by using data analysis program BIAevaluation 3.2RC1 (Biacore AB). Kinetic rate constants were determined by fitting the corrected response data to a simple 1 : 1 (Hill–Langmuir binding isotherm model using BIAevaluation 3.2RC1 software).

Co-immunoprecipitation of PfClpQY complex in the parasite lysate. Infected RBCs were collected from synchronized parasite culture (late-trophozoite stage), suspended in 1 $\times$ PBS pH 7.4 containing cleavable protein cross-linker DTSSP (Pierce Biotechnology Inc., Rockford, IL, USA) (final concentration 2 mM) and incubated for 2 h on ice. The parasites were harvested by lysis of the infected RBCs by 0.15 % saponin in RPMI for 10 min on ice. Parasite pellet was suspended in TEN buffer (Tris 50 mM pH 7.4, 20 mM EDTA) containing protease-inhibitor cocktail (Roche, Indianapolis, IN, USA) and then lysed by three freeze-thaw cycles. The lysate was clarified by centrifugation at 12 000 $\times$ *g* for 30 min at 4 °C and pre-cleared with Protein-A Sepharose beads. The pre-cleared parasite extract was incubated with Protein-A Sepharose beads having immobilized anti-PfClpY antibodies (anti-PfClpY-Protein A Sepharose beads) for 2 h at 4 °C with gentle agitation. After incubation the beads were washed extensively in TEN buffer containing 0.1% Tween-20. The immune complex were dissociated by boiling the beads in SDS-PAGE buffer and centrifuged to separate the beads. The supernatant was separated on SDS-PAGE and analyzed by immunoblotting using anti-PfClpQ antibodies. In control reactions, the anti-PfClpY antibodies were replaced with control antibodies (pre-immune) or with antibodies against a non-specific *P. falciparum* protein, PfAARP.[41]

Mitochondria membrane potential assay. The mitochondrial membrane potential was assessed in the parasite using MitoProbe JC-1 Assay Kit for Flow Cytometry (Molecular Probe, Eugene, OR, USA), this kit uses a unique cationic dye, JC-1 (5,5′,6,6′-tetrachloro-1,1′,3,3′- tetraethylbenzimidazolylcarbocyanine iodide), that remains in monomeric form in the cytoplasm and has a green fluorescence (525 nm). However, the membrane potential of functional mitochondria establishes a negative charge that allows the lipophilic dye to accumulate and form aggregates in the mitochondria, which have red fluorescence (590 nm). Infected RBCs were collected from parasite cultures in control and experimental sets at different time points and incubated with JC-1 dye (at a final concentration. of 10 μM) for 30 min at 37 °C. Cells were washed with PBS and analyzed by flow cytometry using FACSCalibur flow cytometer and CellQuestPro software (Becton Dickinson, San Jose, CA, USA). The infected RBCs were analyzed using green (488 nm) and red (635 nm) filters. Ratio of JC-1 (red)/JC-1 (green) were calculated to assess the loss of mitochondrial membrane potential. The JC-1-stained uninfected RBCs were used as background controls.

Caspase-like cysteine protease-activation assay. A specific caspase-inhibitor CaspACE FITC–VAD–FMK *In Situ* Marker (Promega, Mannheim, Germany) was used to assess activation of Caspase-like cysteine protease activity in the parasite, following manufacturer's instructions. Briefly, the infected RBCs were collected from parasite cultures in control and experimental sets at different time points and incubated with 10 μM of CaspACE FITC–VAD–FMK for 30 min at 37 °C followed by washing with 1 $\times$ PBS. The stained samples were analyzed by flow cytometer using FACSCalibur flow cytometer and CellQuestPro software (Becton Dickinson) to assess fluorescence staining of infected RBCs. Uninfected RBCs were used as background control and parasite culture treated with solvent alone was used as negative controls.

Terminal deexynucleotidyl transferase (TdT) mediated dUTP nick-end labeling (TUNEL). The DNA fragmentation in the parasite was assessed by TUNEL using In Situ Cell Death Detection Kit, TMR Red (Roche Applied Science), following manufacturer's instructions. Briefly, the infected RBCs from control and experimental wells were collected at different time points, fixed with 4% paraformaldehyde (PFA) for 1 h and washed with 1 $\times$ PBS. Subsequently, the cells were incubated with a mixture of TdT enzyme and TMR Red-labeled dUTP for 1 h at 37 °C. The labeled parasites were observed under fluorescence microscope and percentage of TUNEL-positive parasites was calculated. Untreated parasites and parasites treated with DNase were used as negative and positive controls, respectively.

Fluorescence microscopy. *P. falciparum* cultures stained with JC-1 dye and by TUNEL assay were visualized by fluorescence microscopy. These parasites were stained with DAPI at a final concentration of 2 μg/ml for 30 min at 37 °C before imaging. The stained parasites were viewed using a Nikon TE 2000-U fluorescence microscope or Nikon A1R confocal laser scanning microscope (Nikon, Tokyo, Japan). For TUNEL assay, total number of parasites was counted by nuclear staining and percentage of TUNEL-positive parasites was calculated. To study uptake of peptide in the parasite, the peptide was labeled with EZ-Link Sulfo-NHS-LC-LC-Biotin (Pierce) following manufacturer's instruction; the treated parasite were fixed in 4% PFA, stained with streptavidin-FITC and MitoTracker Red CMXRos (Invitrogen) as described earlier[15] and the parasite was visualized using fluorescence microscope.

Conflict of Interest

The authors declare no conflict of interest.

Acknowledgements. We thank Rotary blood bank, New Delhi for providing the human RBCs. SR and MA are supported by research fellowship from ICMR, Govt. of India. SJ is supported by research fellowship from CSIR, Govt. of India. The research work in AM's laboratory is supported by Department of Biotechnology, Govt. of India.

1. Snow RW, Guerra CA, Noor AM, Myint HY, Hay SI. The global distribution of clinical episodes of *Plasmodium falciparum* malaria. *Nature* 2005; **434**: 214–217.
2. Hay SI, Guerra CA, Gething PW, Patil AP, Tatem AJ, Noor AM *et al.* A world malaria map: *Plasmodium falciparum* endemicity in 2007. *PLoS Med* 2009; **6**: e1000048.
3. Waller RF, McFaddenm GI. The apicoplast: a review of the derived plastid of apicomplexan parasites. *Curr Issues Mol Biol* 2005; **7**: 57–79.
4. Goodman CD, Su V, McFadden GI. The effects of anti-bacterials on the malaria parasite *Plasmodium falciparum*. *Mol Biochem Parasitol* 2007; **152**: 181–191.
5. Dahl EL, Rosenthal PJ. Apicoplast translation, transcription and genome replication: targets for antimalarial antibiotics. *Trends Parasitol* 2008; **24**: 279–284.
6. De Mot R, Nagy I, Walz J, Baumeister W. Proteasomes and other self compartmentalizing proteases in prokaryotes. *Trends Microbiol* 1999; **7**: 88–92.
7. Ciechanover A. Intracellular protein degradation: from a vague idea thru the lysosome and the ubiquitin-proteasome system and onto human diseases and drug targeting. *Cell Death Differ* 2005; **12**: 1178–1190.
8. Bochtler M, Hartmann C, Song HK, Bourenkov GP, Bartunik HD, Huber R. The structures of HslU and the ATP-dependent protease HslU-HslV. *Nature* 2000; **403**: 800–805.
9. Seong IS, Kang MS, Choi MK, Lee JW, Koh OJ, Wang J *et al.* The C-terminal tails of HslU ATPase act as a molecular switch for activation of HslV peptidase. *J Biol Chem* 2002; **277**: 25976–25982.
10. Navon A, Ciechanover A. The 26 S proteasome: from basic mechanisms to drug targeting. *J Biol Chem* 2009; **284**: 33713–33718.
11. Fribley A, Wang CY. Proteasome inhibitor induces apoptosis through induction of endoplasmic reticulum stress. *Cancer Biol Ther* 2006; **5**: 745–748.
12. MacLaren AP, Chapman RS, Wyllie AH, Watson CJ. p53-dependent apoptosis induced by proteasome inhibition in mammary epithelial cells. *Cell Death Differ* 2001; **8**: 210–218.
13. Kanemori M, Yanagi H, Yura T. The ATP-dependent HslVU/ClpQY protease participates in turnover of cell division inhibitor SulA in *Escherichia coli*. *J Bacteriol* 1999; **181**: 3674–3680.
14. Ramasamy G, Gupta D, Mohmmed A, Chauhan VS. Characterization and localization of *Plasmodium falciparum* homolog of prokaryotic ClpQ/HslV protease. *Mol Biochem Parasitol* 2007; **152**: 139–148.
15. Rathore S, Sinha D, Asad M, Böttcher T, Afreen F, Chauhan VS *et al.* A cyanobacterial serine protease of *Plasmodium falciparum* is targeted to the apicoplast and plays important role in its growth and development. *Mol Microbiol* 2010; **77**: 873–890.
16. Tschan S, Kreidenweiss A, Stierhof YD, Sessler N, Fendel R, Mordmüller B. Mitochondrial localization of the threonine peptidase PfHslV, a ClpQ ortholog in *Plasmodium falciparum*. *Int J Parasitol* 2010; **40**: 1517–1523.
17. Dhawan S, Dua M, Chishti AH, Hanspal M. Ankyrin peptide blocks falcipain-2-mediated malaria parasite release from red blood cells. *J Biol Chem* 2003; **278**: 30180–30186.
18. Korde R, Bhardwaj A, Singh R, Srivastava A, Chauhan VS, Bhatnagar RK *et al.* A prodomain peptide of Plasmodium falciparum cysteine protease (falcipain-2) inhibits malaria parasite development. *J Med Chem* 2008; **51**: 3116–3123.
19. Subramaniam S, Mohmmed A, Gupta D. Molecular modeling studies of the interaction between *Plasmodium falciparum* HslU and HslV subunits. *J Biomol Struc Dyn* 2008; **26**: 473–479.
20. Kheifets V, Mochly-Rosen D. Insight into intra- and inter-molecular interactions of PKC: design of specific modulators of kinase function. *Pharmacol Res* 2007; **55**: 467–476.
21. Caputo GA, Litvinov RI, Li W, Bennett JS, Degrado WF, Yin H. Computationally designed peptide inhibitors of protein-protein interactions in membranes. *Biochemistry* 2008; **47**: 8600–8606.
22. Hernáez B, Tarragó T, Giralt E, Escribano JM, Alonso C. Small peptide inhibitors disrupt a high-affinity interaction between cytoplasmic dynein and a viral cargo protein. *J Virol* 2010; **84**: 10792–10801.

23. Jean L, Hackett F, Martin SR, Blackman MJ. Functional characterization of the propeptide of *Plasmodium falciparum* subtilisin-like protease-1. *J Biol Chem* 2003; **278**: 28572–28579.
24. Li Z, Lindsay ME, Motyka SA, Englund PT, Wang CC. Identification of a bacterial-like HslVU protease in the mitochondria of *Trypanosoma brucei* and its role in mitochondrial DNA replication. *PLoS Pathog* 2008; **4**: e1000048.
25. Mather MW, Henry KW, Vaidya AB. Mitochondrial drug targets in apicomplexan parasites. *Curr Drug Targets* 2007; **8**: 49–60.
26. Feagin JE. The 6-kb element of *Plasmodium falciparum* encodes mitochondrial cytochrome genes. *Mol Biochem Parasitol* 1992; **52**: 145.
27. Suplick K, Morrisey J, Vaidya AB. Complex transcription from the extrachromosomal DNA encoding mitochondrial functions of *Plasmodium yoelii*. *Mol Cell Biol* 1990; **10**: 6381–6388.
28. Bender A, van Dooren GG, Ralph SA, McFadden GI, Schneider G. Properties and prediction of mitochondrial transit peptides from *Plasmodium falciparum*. *Mol Biochem Parasitol* 2003; **132**: 59–66.
29. Bota DA, Ngo JK, Davies KJ. Down regulation of the human Lon protease impairs mitochondrial structure and function and causes cell death. *Free Radic Biol Med* 2005; **38**: 665–677.
30. Meslin B, Barnadas C, Boni V, Latour C, De Monbrison F, Kaiser K *et al.* Features of apoptosis in *Plasmodium falciparum* erythrocytic stage through a putative role of PfMCA1 metacaspase-like protein. *J Infect Dis* 2007; **195**: 1852–1859.
31. Ch'ng JH, Kotturi SR, Chong AG, Lear MJ, Tan KS. A programmed cell death pathway in the malaria parasite *Plasmodium falciparum* has general features of mammalian apoptosis but is mediated by clan CA cysteine proteases. *Cell Death Dis* 2010; **1**: e26.
32. Das M, Mukherjee SB, Shaha C. Hydrogen peroxide induces apoptosis-like death in *Leishmania donovani* promastigotes. *J Cell Sci* 2001; **114** (Part 13): 2461–2469.
33. Lee N, Bertholet S, Debrabant A, Muller J, Duncan R, Nakhasi HL. Programmed cell death in the unicellular protozoan parasite *Leishmania*. *Cell Death Differ* 2002; **9**: 53–64.
34. Madeo F, Herker E, Maldener C, Wissing S, Lächelt S, Herlan M *et al.* A caspase-related protease regulates apoptosis in yeast. *Mol Cell* 2002; **9**: 911–917.
35. Trager W, Jensen JB. Human malaria parasites in continuous culture. *Science* 1976; **193**: 673–675.
36. Lambros C, Vanderberg JP. Synchronization of *Plasmodium falciparum* erythrocytic stage in culture. *J Parasitol* 1979; **65**: 418–420.
37. Schlichtherle M, Wahlgren M, Perlmann H, Scherf A. *Methods in Malaria Research*. MR4/ATCC: Manassas, 2000.
38. Dasaradhi PV, Mohmmed A, Kumar A, Hossain MJ, Bhatnagar RK, Chauhan VS, VA*et al.* A role of falcipain-2, principal cysteine proteases of *Plasmodium falciparum* in merozoite egression. *Biochem Biophys Res Commun* 2005; **336**: 1062–1068.
39. Blair PL, Witney A, Haynes JD, Moch JK, Carucci DJ, Adams JH. Transcripts of developmentally regulated *Plasmodium falciparum* genes quantified by realtime RT-PCR. *Nucleic Acids Res* 2002; **30**: 2224–2231.
40. Ramachandran R, Hartmann C, Song HK, Huber R, Bochtler M. Functional interactions of HslV (ClpQ) with the ATPase HslU (ClpY). *Proc Natl Acad Sci* 2002; **99**: 7396–7401.
41. Wickramarachchi T, Devi YS, Mohmmed A, Chauhan VS. Identification and characterization of a novel *Plasmodium falciparum* merozoite apical protein involved in erythrocyte binding and invasion. *PLoS One* 2008; **3**: e1732.

Supplementary Information accompanies the paper on Cell Death and Disease website (http://www.nature.com/cddis)